Journal of Solid State Chemistry **147,** 552–560 (1999)
Article ID jssc.1999.8416, available online at http://www.idealibrary.com on IDEAL®

A New Vanadium Oxide Bronze: $[NH_3(CH_2)_6NH_3]_{10}[V_{15}O_{37}(Cl)]_2[V_{15}O_{36}(Cl)](OH)_3(H_2O)_3$ with Clusters $[V_{15}O_{36}(Cl)]^{5-}$ and $[V_{15}O_{37}(Cl)]^{6-}$ Textured by Diaminohexane

Thierry Drezen and Marcel Ganne[1]

Institut des matériaux de Nantes, Laboratoire de chimie des solides, UMR CNRS N° 110, B. P. 32229, 2 rue de la Houssinière, 44322 Nantes Cedex 03, France

Received February 22, 1999; in revised form June 4, 1999; accepted June 28, 1999

A novel mesostructured mixed-valence polyoxovanadate with formula $[NH_3(CH_2)_6NH_3]_{10}[V_{15}O_{37}(Cl)]_2[V_{15}O_{36}(Cl)](OH)_3(H_2O)_3$ was synthesized hydrothermally under autogeneous pressure at 443 K for 5 days from an aqueous mixture of $NH_2(CH_2)_6NH_2$ and V_2O_5 in acidic HCl (1 M) medium. Its structure was solved from single-crystal X-ray diffraction data at room temperature. It crystallizes in the orthorhombic symmetry (space group *Pnma*) with $a = 23.616(5)$, $b = 44.785(9)$, $c = 18.568(4)$ Å, $V = 19638.3(5)$ Å^3, and $Z = 4$. Two types of polyoxovanadate clusters, $[V_{15}O_{37}(Cl)]^{6-}$ and $[V_{15}O_{36}(Cl)]^{5-}$, have been characterized, around which the stacking of hexanediamine dications is different. XPS measurements are in reasonable agreement with the calculated average vanadium valence state of 4.60 ± 0.1 in this hybrid compound. All things being similar, hexanediamine appears to be slightly less reducing than octyldiamine and therefore has been placed below octyldiamine in a phenomenological diagram implying the "effective" redox potential of diamines which have to be compared with that of V^V/V^{IV} couple in the solid. © 1999 Academic Press

Key Words: **vanadium–oxygen clusters; mixed-valence; hybrid compound; diamine "effective" redox potential; XPS analysis.**

INTRODUCTION

In the past years, the hydrothermal technique combined with the templating effect of various organic cations has been extensively used for synthesis of zeolite molecular sieves (1, 2). More recently the silica-based mesoporous MCM-41 was obtained by use of amphiphilic cations (3, 4). Since then, this discovery has prompted a renewed interest for soft chemistry routes, among which is the use of organic templates. In this field, new series of molybdenum and vanadium phosphates and phosphonates containing amines or diamines with 1-D, 2-D, and 3-D open-framework structures were prepared (5–11). For a few years, the texturing effect of diamines has made it possible to synthesize new vanadium or molybdenum oxide structures containing organic dications. So far, the chemical behavior is not fully elucidated for these new intercalated transition-metal oxides, whose framework dimensionalities seem to vary, especially as a function of pH and diamine length. Furthermore, the chemistry of these new organic–inorganic hybrids is by far very versatile as it depends on several hard-to-control parameters, such as composition, absolute and relative concentrations, temperature, pH, time, and heating and cooling rates. Hence, the results can be hardly predictable. Possibly, two phases, reduced and unreduced, may coexist as it was recently found in the system molybdenum oxide textured by ethylenediamine (12).

Our research thematic concerns investigations of the diamine length influence on dimensionality of vanadium and molybdenum oxide frameworks. Recently, we described a new mixed-valence vanadium oxide textured by octyldiammonium cations (13, 14). The inorganic framework is built up from vanadium–oxygen clusters encapsulating a Cl^- anion, $[V_{15}O_{36}(Cl)]^{6-}$, first described by Müller *et al.* (15, 16) and later by Shao *et al.* (17) for the related $[V_{15}O_{36}(Cl)]^{10-}$ prepared in basic medium without template.

In this paper we report on the characterization of a novel hybrid vanadium oxide templated by hexanediamine which contains two types of vanadium–oxygen clusters, namely $[V_{15}O_{37}(Cl)]^{6-}$ and $[V_{15}O_{36}(Cl)]^{5-}$.

EXPERIMENTAL

Synthesis

The available commercial reactants V_2O_5, 1-6 diaminohexane, HCl (1 M) were mixed with water in the respective molar ratios 1:1.5:1.8:239. This unstirred mixture was readily transferred into a Teflon-lined stainless-steel home-made autoclave. The initial pH value was 2.5. The mixture occupied 80% of the autoclave volume. After gradual heating up to 443 K, this temperature was maintained constant for 5 days. After that, the temperature was

[1] To whom correspondence should be addressed. E-mail: ganne@cnrs-imn.fr. Fax: (33) 02 40 37 39 95.

0022-4596/99 $30.00

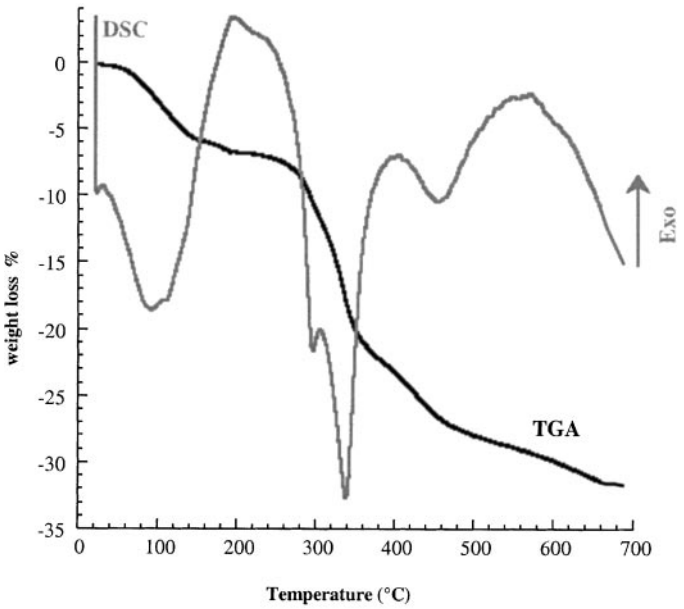

FIG. 1. TGA and DSC curves of $[NH_3(CH_2)_6NH_3]_{10}[V_{15}O_{37}(Cl)]_2[V_{15}O_{36}(Cl)](OH)_3(H_2O)_3$ (heating rate 300 K/h).

decreased to room temperature for 15 h. The final pH of the mixture was close to 6.5 at room temperature. These synthesis conditions have been quite similar to those carried out for $[NH_3(CH_2)_8NH_3]_3[V_{15}O_{36}(Cl)](NH_3)_6(H_2O)_3$ (13). The solid prepared under autogeneous pressure contained a mixture of black single crystals and black powder.

A small amount of hand-picked crystals was collected for hydrolysis tests and a study by TGA under argon coupled to a mass spectrometer analysis. At room temperature, these single crystals very slowly undergo surface hydration but are quickly hydrolized in water. The TGA analysis shown in Fig. 1 exhibits a first loss of 5.5% below 393 K, attributed to surface hydration water. A second loss of 1.8% was observed between 393 and 483 K and was related to constituent water and hydroxyl groups. The decomposition of hexanediammonium cations was observed between 493 and 743 K and corresponds to a weight loss of 21%. A further loss of about 4% was attributed to chlorine and oxygen removal from the solid to give an unidentified amorphous solid, most likely a vanadium suboxide. Hence, thermal analysis did not make it possible to propose the exact formulation, finally established after a complete structural determination.

Structure Determination

Diffraction data collection was carried out on a STOE Imaging Plate system using the Mo$K\alpha$ X-ray radiation. A total of 66,892 intensities were collected at room temperature and corrected for Lorentz and polarization effects but not for absorption. The averaging in the orthorhombic space group *Pnma* gave 9689 independent reflections, among which 6731 obeyed the criterion $I > 2\sigma(I)$. The structure was solved by combining direct methods and Fourier syntheses using the XS and XL routines of the SHELXTL program chain version 5 (18). No attempt was made for positioning hydrogen atoms because of the already high number of atomic parameters to be refined in that very large unit cell. Only vanadium, chloride, and oxygen atoms were anisotropically refined, whereas carbon and nitrogen atoms were isotropically refined. Crystal and intensity collection data as well as significant refinement parameters are given in Table 1. Refining attempts in the other allowed space group $Pn2_1a$ did not give satisfactory results. Atomic coordinates and equivalent temperature factors are given in Table 2. Accordingly, the formulation of the new hybrid

TABLE 1
Crystal, Collection, and Refinement Data of $[NH_3(CH_2)_6NH_3]_{10}[V_{15}O_{37}(Cl)]_2[V_{15}O_{36}(Cl)](OH)_3(H_2O)_3$

	Crystal data
Chemical formula	$[NH_3(CH_2)_6NH_3]_{10}[V_{15}O_{37}(Cl)]_2$ $[V_{15}O_{36}(Cl)](OH)_3(H_2O)_3$
Formula mass (amu)	5445.96
Crystal system	Orthorhombic
Space group	*Pnma*
Z	4
Description	Black plate-like crystal
Size (mm)	$0.75 \times 0.2 \times 0.12$
Temperature	293 K
a (Å)	23.616(5)
b (Å)	44.785(9)
c (Å)	18.568(4)
α (°)	90.0
β (°)	90.0
γ (°)	90.0
V (Å^3)	19638.3(5)
ρ calc (g cm^{-3})	1.84
μ(Mo$K\alpha$) (mm^{-1})	2.16
	Data collection
Diffractometer type	STOE Imaging Plate
Radiation	Mo$K\alpha$, $\lambda = 0.7107$ Å
θ range (°)	$2.3 \leq \theta \leq 42.0$
Index ranges	$-23 \leq h \leq 23$, $-44 \leq k \leq 44$, $-16 \leq l \leq 17$
Collected reflections	66892
Independent reflections	9689 [R(Int) = 0.0609]
Observed reflections with $I > 2\sigma(I)$	6731
	Refinement (on F^2)
Atomic scattering factors	Neutral atoms from SHELXTL sofware
No. of variables	915
$R_1(F)$	0.073
w$R_2(F^2)$	0.135
Goodness-of-fit on F^2	1.75
Extinction coefficient	0.0014(1)
Largest diff. peak and hole	2.5 and -1.4 e Å^{-3}

TABLE 2
Positional and Thermal Parameters for $[NH_3(CH_2)_6NH_3]_{10}[V_{15}O_{37}(Cl)]_2[V_{15}O_{36}(Cl)](OH)_3(H_2O)_3$

Atom	Wyckoff position	x	y	z	U (eq)[a] (Å^2)
V(1)	8*d*	0.1802(1)	0.0578(1)	0.7756(2)	0.0215(9)
V(2)	8*d*	0.0686(1)	0.0345(1)	0.6585(2)	0.0234(9)
V(3)	8*d*	0.0365(1)	0.0855(1)	0.5643(2)	0.0294(9)
V(4)	8*d*	0.2612(1)	0.0088(1)	0.5471(2)	0.0237(9)
V(5)	8*d*	0.3192(1)	0.0685(1)	0.5488(2)	0.0242(9)
V(6)	8*d*	0.2929(1)	0.0537(1)	0.7013(2)	0.0207(9)
V(7)	8*d*	0.1738(1)	0.0027(1)	0.6859(2)	0.0231(9)
V(8)	8*d*	0.1133(1)	0.0193(1)	0.5121(2)	0.0228(9)
V(9)	8*d*	0.0914(1)	0.1108(1)	0.7002(2)	0.0256(9)
V(10)	8*d*	0.2735(1)	0.1190(1)	0.7789(2)	0.033(1)
V(11)	8*d*	0.2270(1)	0.1224(1)	0.4683(2)	0.029(1)
V(12)	8*d*	0.2879(1)	0.1263(1)	0.6050(2)	0.030(1)
V(13)	8*d*	0.1242(1)	0.0912(1)	0.4234(2)	0.030(1)
V(14)	8*d*	0.1382(1)	0.1445(1)	0.5702(2)	0.032(1)
V(15)	8*d*	0.2094(1)	0.0445(1)	0.42716	0.027(1)
V(16)	8*d*	0.1551(1)	0.1889(1)	1.0432(2)	0.048(1)
V(17)	8*d*	0.0373(1)	0.1885(1)	0.1613(3)	0.055(1)
V(18)	8*d*	0.1188(1)	0.2129(1)	0.8994(3)	0.052(1)
V(19)	4*c*	− 0.0166(2)	0.2500	0.9148(4)	0.052(1)
V(20)	8*d*	0.0141(2)	0.1890(1)	0.9717(3)	0.046(1)
V(21)	4*c*	0.2081(2)	0.2500	1.0292(4)	0.057(1)
V(22)	8*d*	− 0.0618(2)	0.2125(1)	0.0815(4)	0.066(2)
V(23)	8*d*	0.1508(2)	0.2110(2)	1.1894(4)	0.072(2)
V(24)	4*c*	0.0169(4)	0.2500	1.2281(5)	0.084(3)
Cl(1)	4*c*	0.0717(2)	0.2500	1.0569(5)	0.064(3)
Cl(2)	8*d*	0.1798(4)	0.0715(1)	0.5939(3)	0.037(2)
O(1)	8*d*	0.3112(4)	0.0879(3)	0.6411(7)	0.025(3)
O(2)	8*d*	0.1173(4)	0.0060(3)	0.6121(8)	0.020(3)
O(3)	8*d*	0.0560(5)	0.0914(3)	0.4731(7)	0.034(4)
O(4)	8*d*	0.0142(5)	0.0154(3)	0.6845(8)	0.032(4)
O(5)	8*d*	0.0541(5)	0.0441(3)	0.5599(8)	0.025(4)
O(6)	8*d*	0.2910(5)	0.1048(3)	0.5103(8)	0.026(3)
O(7)	8*d*	0.2271(5)	− 0.0097(3)	0.6193(8)	0.022(3)
O(8)	8*d*	0.1929(5)	0.0110(3)	0.4913(8)	0.024(3)
O(9)	8*d*	0.2280(5)	0.0293(3)	0.7279(8)	0.021(3)
O(10)	8*d*	0.1362(5)	0.0912(3)	0.7611(7)	0.031(4)
O(11)	8*d*	0.1276(5)	0.0482(3)	0.4359(7)	0.023(3)
O(12)	8*d*	0.2790(5)	0.0436(3)	0.4822(7)	0.024(3)
O(13)	8*d*	0.0480(5)	0.1281(3)	0.7534(9)	0.041(4)
O(14)	8*d*	0.3462(5)	0.0430(3)	0.7510(7)	0.025(3)
O(15)	8*d*	0.1788(5)	0.0483(3)	0.8605(7)	0.026(4)
O(16)	8*d*	0.1477(5)	0.1405(3)	0.6755(8)	0.037(4)
O(17)	8*d*	0.1640(5)	− 0.0258(3)	0.7357(8)	0.031(4)
O(18)	8*d*	0.1458(5)	0.1267(3)	0.4734(8)	0.028(4)
O(19)	8*d*	0.0725(5)	0.1202(3)	0.5993(8)	0.030(4)
O(20)	8*d*	− 0.0308(5)	0.0895(3)	0.5663(8)	0.038(4)
O(21)	8*d*	0.2510(6)	0.1452(3)	0.4096(8)	0.041(4)
O(22)	8*d*	0.1061(6)	0.0996(3)	0.3429(8)	0.043(4)
O(23)	8*d*	0.2211(5)	0.1422(3)	0.5585(7)	0.027(4)
O(24)	8*d*	0.2079(5)	0.0871(3)	0.4194(8)	0.032(4)
O(25)	8*d*	0.0512(5)	0.0748(3)	0.6724(7)	0.022(3)
O(26)	8*d*	0.3043(5)	0.0333(3)	0.6083(7)	0.022(3)
O(27)	8*d*	0.0782(5)	− 0.0070(3)	0.4721(7)	0.031(4)
O(28)	8*d*	0.0963(5)	0.1835(3)	0.9761(9)	0.045(4)
O(29)	8*d*	0.1227(5)	0.0332(3)	0.7308(7)	0.026(4)
O(30)	8*d*	0.3847(5)	0.0682(3)	0.5241(9)	0.037(4)
O(31)	8*d*	0.3010(5)	− 0.0161(3)	0.5110(8)	0.033(4)
O(32)	8*d*	0.2261(6)	0.0305(3)	0.3496(8)	0.042(4)
O(33)	8*d*	0.0376(6)	0.2179(3)	0.8986(9)	0.045(4)
O(34)	8*d*	0.1181(6)	0.1774(3)	0.5565(9)	0.050(5)
O(35)	8*d*	0.3415(6)	0.1487(3)	0.5983(9)	0.041(4)
O(36)	4*c*	0.1306(8)	0.2500	0.864(1)	0.048(6)
O(37)	8*d*	0.1950(6)	0.2182(4)	1.103(1)	0.051(5)
O(38)	8*d*	− 0.0107(6)	0.1600(4)	0.932(1)	0.058(5)
O(39)	8*d*	− 0.0445(6)	0.2183(4)	0.978(1)	0.055(5)
O(40)	8*d*	0.1782(6)	0.2170(4)	0.968(1)	0.053(5)
O(41)	8*d*	0.1103(6)	0.1816(4)	1.123(1)	0.057(6)
O(42)	8*d*	0.1960(6)	0.1608(4)	1.033(1)	0.055(5)
O(43)	8*d*	0.0041(6)	0.1828(4)	1.067(1)	0.056(5)
O(44)	4*c*	0.2740(9)	0.2500	1.015(1)	0.063(7)
O(45)	8*d*	0.1372(7)	0.1911(4)	0.837(1)	0.060(5)
O(46)	4*c*	− 0.0574(9)	0.2500	0.846(1)	0.072(7)
O(47)	8*d*	0.0228(7)	0.1597(4)	0.210(1)	0.065(6)
O(48)	4*c*	− 0.0868(9)	0.2500	0.097(2)	0.080(8)
O(49)	8*d*	− 0.1163(7)	0.1923(5)	0.093(1)	0.078(8)
O(50)	8*d*	0.1859(9)	0.1897(6)	1.243(1)	0.081(8)
O(51)	4*c*	0.1656(7)	0.2500	1.221(1)	0.064(7)
O(52)	8*d*	− 0.0254(9)	0.2150(4)	0.177(1)	0.066(5)
O(53)	8*d*	0.2570(5)	0.1377(3)	0.698(1)	0.030(4)
O(54)	8*d*	0.2507(4)	0.0801(3)	0.768(1)	0.024(3)
O(55)	8*d*	0.34293(5)	0.1208(3)	0.794((1)	0.044(4)
O(56)	8*d*	0.2395(6)	0.1350(3)	0.847(1)	0.045(4)
O(57)	8*d*	0.0753(7)	0.2156(4)	1.225(1)	0.065(5)
O(58)	4*c*	− 0.0019(9)	0.2500	1.310(1)	0.068(7)
O(59)	8*d*	0.0067(9)	0.1888(7)	0.754(1)	0.092(9)
O(60)	8*d*	0.0874(9)	0.0164(7)	0.313(1)	0.082(9)
O(61)	8*d*	0.3922(9)	0.1682(7)	0.726(1)	0.087(9)
N(1)	8*d*	0.3510(7)	0.0148(4)	0.385(1)	0.033(4)
N(2)	8*d*	− 0.0617(7)	0.0826(4)	0.737(1)	0.039(5)
N(3)	8*d*	0.1019(8)	− 0.1365(5)	0.969(1)	0.055(6)
N(4)	8*d*	0.0121(7)	− 0.0382(5)	0.580(1)	0.043(5)
N(5)	8*d*	0.1247(8)	0.1318(4)	0.893(1)	0.054(6)
N(6)	8*d*	0.1784(9)	0.0211(6)	0.217(1)	0.076(6)
N(7)	8*d*	0.1992(7)	− 0.0385(4)	0.398(1)	0.046(5)
N(8)	8*d*	0.2874(9)	0.1612(9)	1.268(2)	0.151(5)
N(9)	8*d*	0.0930(9)	0.1685(9)	0.354(2)	0.143(1)
N(10)	8*d*	0.2811(9)	0.1871(6)	0.909(2)	0.085(7)
C(1)	8*d*	0.411(1)	0.013(1)	0.419(1)	0.049(6)
C(2)	8*d*	0.445(1)	− 0.007(1)	0.370(1)	0.047(6)
C(3)	8*d*	0.504(1)	− 0.012(1)	0.401(1)	0.049(6)
C(4)	8*d*	− 0.039(1)	0.034(1)	0.850(1)	0.048(6)
C(5)	8*d*	− 0.014(1)	0.065(1)	0.848(1)	0.049(6)
C(6)	8*d*	− 0.053(1)	0.089(1)	0.815(1)	0.040(6)
C(7)	8*d*	0.060(1)	− 0.119(1)	0.925(1)	0.056(7)
C(8)	8*d*	0.086(1)	− 0.112(1)	0.852(1)	0.053(7)
C(9)	8*d*	0.044(1)	− 0.093(1)	0.809(1)	0.069(6)
C(10)	8*d*	0.067(1)	− 0.087(1)	0.732(1)	0.050(7)
C(11)	8*d*	0.027(1)	− 0.066(1)	0.691(1)	0.054(7)
C(12)	8*d*	0.049(1)	− 0.060(1)	0.617(1)	0.051(7)
C(13)	8*d*	0.129(1)	0.106(1)	0.954(2)	0.10(1)
C(14)	8*d*	0.079(1)	0.106(1)	0.996(2)	0.092(9)
C(15)	8*d*	0.077(2)	0.077(1)	1.036(2)	0.12(1)
C(16)	8*d*	0.112(2)	0.077(1)	1.102(2)	0.14(1)
C(17)	8*d*	0.109(1)	0.046(1)	1.147(2)	0.13(1)
C(18)	8*d*	0.173(1)	0.049(1)	0.196(2)	0.12(1)
C(19)	8*d*	0.173(1)	− 0.067(1)	0.434(2)	0.071(7)

TABLE 2—*Continued*

Atom	Wyckoff position	x	y	z	U (eq)[a] (Å^2)
C(20)	8*d*	0.203(1)	−0.072(1)	0.511(2)	0.087(8)
C(21)	8*d*	0.192(1)	−0.100(1)	0.542(2)	0.10(1)
C(22)	8*d*	0.285(1)	0.101(1)	1.122(2)	0.092(8)
C(23)	8*d*	0.297(2)	0.132(1)	1.153(2)	0.12(1)
C(24)	8*d*	0.271(2)	0.127(1)	1.237(3)	0.14(1)
C(25)	8*d*	0.046(2)	0.183(1)	0.387(3)	0.19(1)
C(26)	8*d*	0.009(2)	0.162(1)	0.412(3)	0.15(1)
C(27)	8*d*	−0.045(3)	0.180(2)	0.466(3)	0.25(2)
C(28)	8*d*	−0.074(3)	0.161(2)	0.475(4)	0.21(2)
C(29)	8*d*	0.389(4)	0.170(2)	0.942(5)	0.35(4)
C(30)	8*d*	0.328(2)	0.180(1)	0.968(2)	0.14(1)

[a] $U(\text{eq}) = \frac{1}{3}\sum_i\sum_j U_{ij}a_i^*a_j^*a_ia_j$.

is established as $[NH_3(CH_2)_6NH_3]_{10}[V_{15}O_{37}(Cl)]_2[V_{15}O_{36}(Cl)](OH)_3(H_2O)_3$. By looking at Table 2 describing the positional and thermal parameters it is clear that most of the atoms have rather high thermal parameters, especially the carbons and a few nitrogens (refined isotropically). Even some vanadium and oxygen atoms which belong to the $[V_{15}O_{36}(Cl)]^{5-}$ cluster exhibit high U_{eq} values. This feature arises probably from some kind of dynamic disorder frequently observed in such mesostructured organic/inorganic hybrids. Because of the high volume cell and of the large number of atoms it is not too surprising to observe disorder. For example several vanadyl groups such as V(24)=O(58) or V(23)=O(50) exhibit most likely orientational disorder. In this structure, bond lengths are affected by a rather important standard deviation (Table 3). However, since no special problems for locating atoms were encountered, it can be concluded that the structural determination is reasonably correct.

DESCRIPTION OF THE CRYSTAL STRUCTURE

This new hybrid exhibits an original three-dimensional assembling whose inorganic framework is built up from two types of slightly different vanadium–oxygen clusters: $[V_{15}O_{37}(Cl)]^{6-}$ (I) and $[V_{15}O_{36}(Cl)]^{5-}$ (II) encapsulating the chloride anion Cl^-. The average distance between Cl and V is about 3.43 ± 0.1 Å, practically the same value found by Müller *et al.* (15). A projection of the structure along [001] is shown in Fig. 2. It is of note that the stacking density varies inside the orthorhombic cell. The central part in the cell implying $[V_{15}O_{37}(Cl)]^{6-}$ clusters is more densely stacked than the other part containing the $[V_{15}O_{36}(Cl)]^{5-}$ polyoxovanadate groups. These differences are reflected on distances between the clusters. In the mirror plane perpendicular to the y axis, the clusters $[V_{15}O_{36}(Cl)]^{5-}$ (II) are separated by a Cl(1)–Cl(1) distance of 13.81(1) Å. In the central part of the unit cell the shorter Cl(2)–Cl(2) distances between the $[V_{15}O_{37}(Cl)]^{6-}$ (I) clusters are found at 11.20(1), 11.76(1), and 13.15(1) Å. Interclusters Cl(2)–Cl(1) distances of 12.01(1), 12.54(1), and 13.03(1) Å are observed. So, clusters (II) are more separated than clusters (I). These later are more densely stacked because of higher volumic density of dications in the central part. It is worth noting

TABLE 3
Selected Bond Lengths (Å) in $[NH_3(CH_2)_6NH_3]_{10}$ $[V_{15}O_{37}(Cl)]_2[V_{15}O_{36}(Cl)](OH)_3(H_2O)_3$

		d (Å)			*d* (Å)			*d* (Å)
V1	O15	1.63(1)	V9	O13	1.62(2)	V17	O47	1.60(2)
V1	O10	1.84(1)	V9	O10	1.78(1)	V17	O41	1.89(2)
V1	O9	1.92(1)	V9	O16	1.94(1)	V17	O57	1.92(2)
V1	O29	1.94(1)	V9	O25	1.94(1)	V17	O52	1.92(2)
V1	O54	1.95(1)	V9	O19	1.97(1)	V17	O43	1.94(2)
V2	O4	1.62(1)	V10	O56	1.66(2)	V18	O45	1.58(2)
V2	O29	1.85(1)	V10	O55	1.67(1)	V18	O36	1.80(1)
V2	O25	1.87(1)	V10	O53	1.76(2)	V18	O40	1.91(2)
V2	O5	1.91(1)	V10	O54	1.83(1)	V18	O33	1.93(1)
V2	O2	1.92(1)	V11	O21	1.60(1)	V18	O28	2.01(2)
V3	O20	1.60(1)	V11	O6	1.88(1)	V19	O46	1.60(3)
V3	O3	1.77(1)	V11	O24	1.88(1)	V19	O33	1.95(1)
V3	O19	1.88(1)	V11	O23	1.90(1)	V19	O33	1.95(1)
V3	O5	1.90(1)	V11	O18	1.93(1)	V19	O39	1.96(2)
V3	O25	2.09(1)	V12	O35	1.62(1)	V19	O39	1.96(2)
V4	O31	1.60(1)	V12	O1	1.92(1)	V20	O38	1.60(2)
V4	O7	1.77(1)	V12	O23	1.93(1)	V20	O43	1.80(2)
V4	O26	1.88(1)	V12	O53	1.95(1)	V20	O39	1.91(2)
V4	O8	1.92(1)	V12	O6	2.00(1)	V20	O33	1.95(2)
V4	O12	2.01(1)	V13	O22	1.60(2)	V20	O28	1.97(1)
V5	O30	1.61(1)	V13	O3	1.86(1)	V21	O44	1.58(2)
V5	O6	1.89(1)	V13	O18	1.91(1)	V21	O40	1.98(2)
V5	O12	1.92(1)	V13	O11	1.94(1)	V21	O40	1.98(2)
V5	O1	1.93(1)	V13	O24	1.98(1)	V21	O37	2.00(2)
V5	O26	1.96(1)	V14	O34	1.57(2)	V21	O37	2.00(2)
V6	O14	1.63(1)	V14	O19	1.97(1)	V22	O49	1.59(2)
V6	O1	1.94(1)	V14	O23	1.97(1)	V22	O48	1.80(1)
V6	O9	1.95(1)	V14	O18	1.97(1)	V22	O39	1.97(2)
V6	O26	1.97(1)	V14	O16	1.98(1)	V22	O52	1.98(2)
V6	O54	1.98(1)	V15	O32	1.62(2)	V22	O43	2.06(2)
V7	O17	1.60(1)	V15	O24	1.91(1)	V23	O50	1.61(2)
V7	O7	1.85(1)	V15	O12	1.94(1)	V23	O51	1.88(1)
V7	O9	1.91(1)	V15	O11	1.94(1)	V23	O57	1.91(2)
V7	O2	1.92(1)	V15	O8	1.95(1)	V23	O37	1.94(2)
V7	O29	2.00(1)	V16	O42	1.60(2)	V23	O41	2.04(2)
V8	O27	1.62(1)	V16	O41	1.84(2)	V24	O58	1.58(3)
V8	O11	1.95(1)	V16	O28	1.88(2)	V24	O57	2.07(2)
V8	O2	1.95(1)	V16	O40	1.95(2)	V24	O57	2.07(2)
V8	O8	1.95(1)	V16	O37	1.96(2)	V24	O52	2.08(2)
V8	O5	1.99(1)				V24	O52	2.08(2)
N1	O12	2.80(1)	N4	O27	2.90(1)	N7	O8	2.81(1)
N1	O17	2.83(1)	N5	O56	2.85(1)	N8	O50	2.75(1)
N2	O14	2.81(1)	N5	O28	2.86(1)	N8	O21	2.86(1)
N2	O55	2.89(1)	N5	O45	2.87(1)	N9	O22	3.11(1)
N3	O49	2.77(1)	N6	O32	2.73(1)	N10	O56	2.79(1)
N3	O35	2.80(1)	N6	O60	2.80(1)			

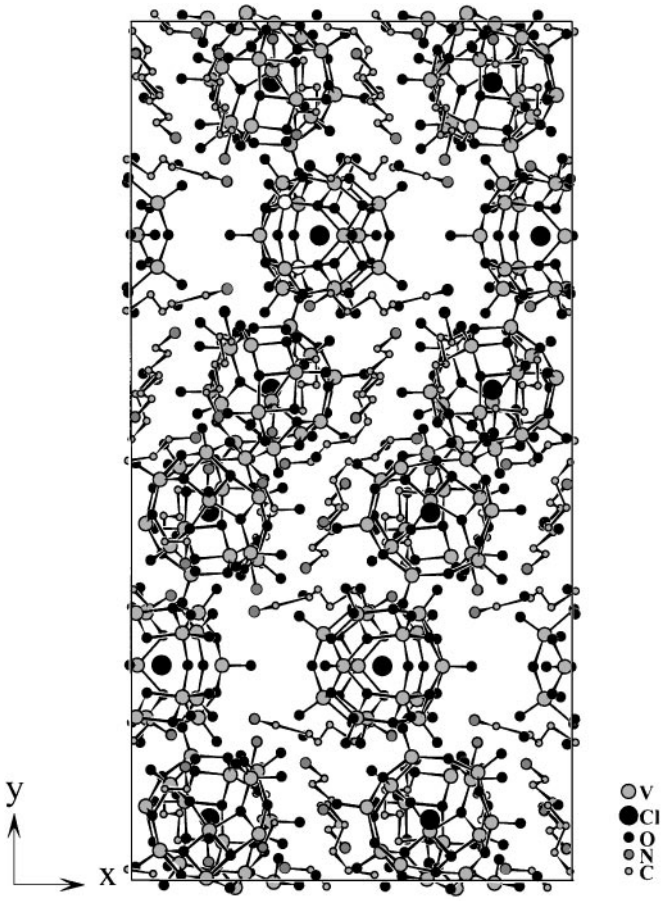

FIG. 2. Projection of the structure of $[NH_3(CH_2)_6NH_3]_{10}[V_{15}O_{37}(Cl)]_2[V_{15}O_{36}(Cl)](OH)_3(H_2O)_3$ along [001].

that orientation of alkyldiammonium chains is also different around clusters (I) and (II). Owing to these differences in compactness for the two parts, the structure could be described as resulting from an intergrowth along [010] between two sublattices, each one containing a different cluster type. In this way the structure can be considered as being two dimensional. Channels between clusters (II) with a diameter size about 5.60 Å (as deduced between O(49) and O(50)) run along the *c* axis and are able to adsorb free water molecules (5.5% in weight) as effectively found from the TGA experiment (Fig. 1).

The two types of clusters, (I) and (II), are depicted in Fig. 3. Although they show similarities, cluster (I) contains a tetrahedral vanadium site (V(10)) which is an original feature. The other vanadium atoms are in square pyramidal sites (symmetry $\approx C_{4v}$), all characterized by the presence of a shorter bond of vanadyl type (V=O) about 1.61 ± 0.02 Å in average length. All the V–O and N–O distances are given in Table 3. From these data it appears to be clear that dications establish hydrogen bonding (N–H $\cdots$ O between 2.73(1) and 2.91(1) Å) with cluster oxygen atoms, as represented in Figs. 4 and 5. The two types of clusters, (I) and (II), share a different number of hydrogen bonds, 8 for cluster (II) and 10 for cluster (I). The water molecules and hydroxide anions are partly located in the neighborhood of clusters (I) in the central part of the cell and partly at the interface between the two sublattices in the channels, on three independent cristallographic (8*d*) Wickoff positions, each one providing a hydrogen bond with cluster (I) oxygens. As proposed above, further place in the channels is available for adsorption of free water molecules.

Individual valence of each vanadium cation has been estimated from calculations of bond valence sums by using the formula of Brown and Altermatt (19). These results are given in Table 4 as well as the average value and its uncertainty inside each cluster (I) and (II). Taking into account the refined crystallographic formula, the average vanadium valence is estimated to be about 4.60 ± 0.1 value, which is

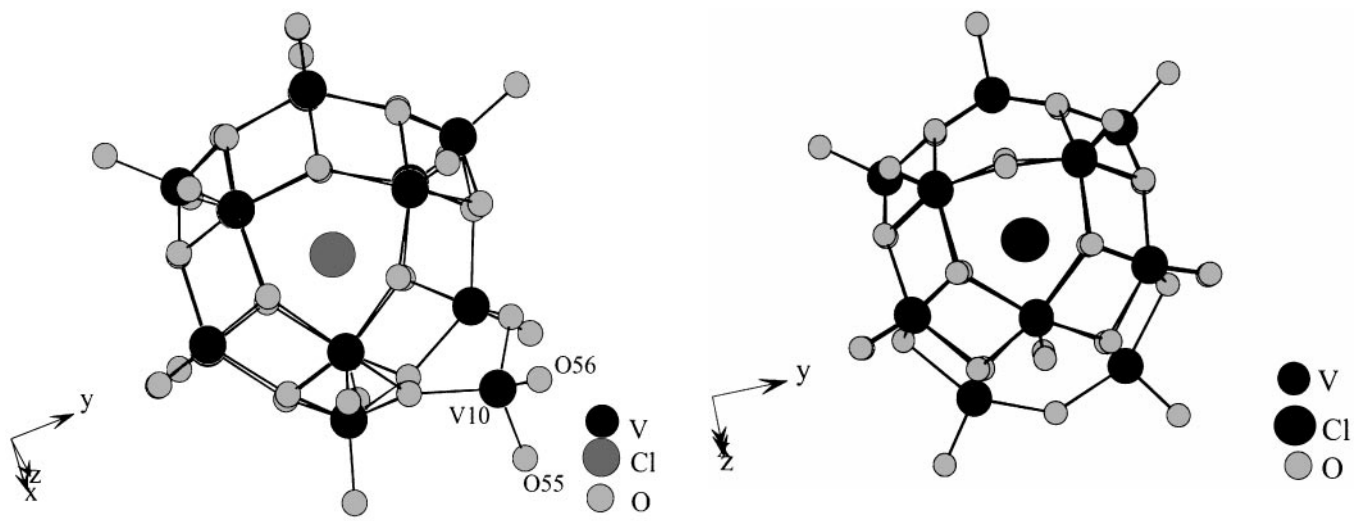

FIG. 3. View of the two types of clusters. (a) Cluster (I): $[V_{15}O_{37}(Cl)]$; (b) cluster (II), $[V_{15}O_{36}(Cl)]$.

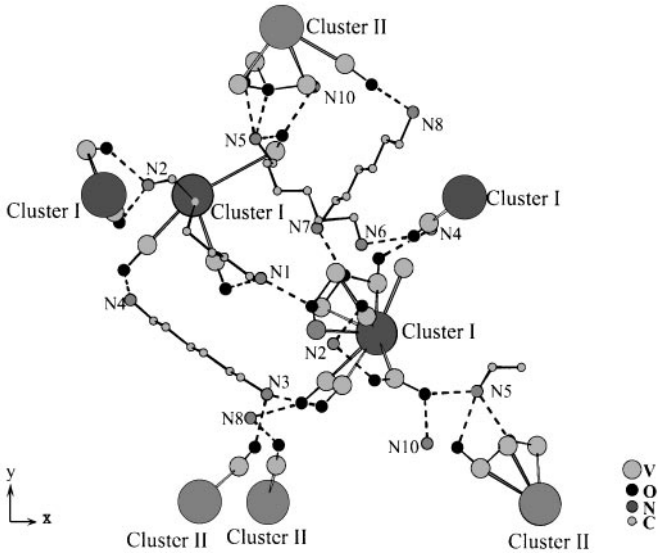

FIG. 4. Arrangement of the hexanediammonium chains around cluster (I), with hydrogen bonds shown as dotted lines.

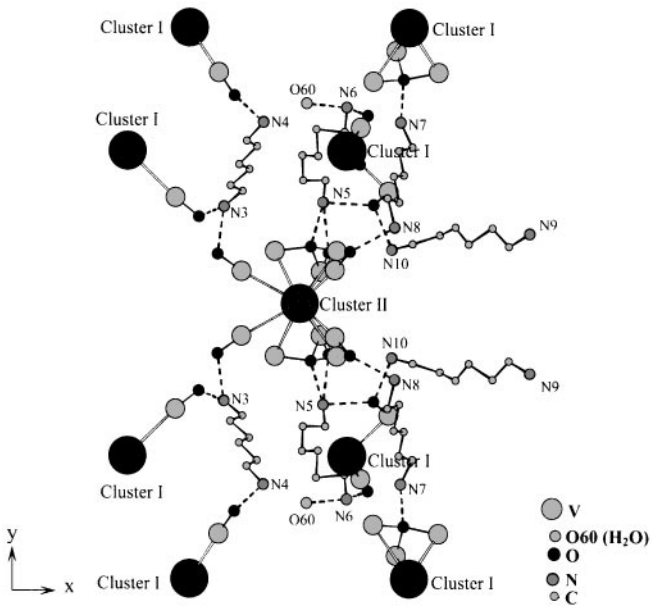

FIG. 5. Arrangement of the hexanediammonium chains around cluster (II), with hydrogen bonds shown as dotted lines.

higher than that found for octyldiamine (4.43 ± 0.02) textured vanadium oxide (13, 14), although these two compounds were prepared under strictly similar conditions.

In order to obtain an independent estimation of this average valence in these two hybrids containing either hexanediammonium or octyldiammonium cations, we have carried out ESCA experiments. XPS measurements were performed on single crystals with the Leybold Heraus apparatus, using the Mg$K\alpha$ X-ray radiation as the excitation source ($E_{MgK\alpha} = 1253.6$ eV). The $2p$ core level excitation of vanadium was especially analyzed. The deconvolution of the $2p_{3/2}$ component of vanadium gave two distributions at 518.73 and 517.44 eV with diaminohexane, respectively 518.49 and 517.22 eV with diaminooctane. The highest value was assigned to V^V and calibrated down to the reference value found in the literature for $2p_{3/2}$ in V_2O_5 (517.4 eV) (20) for which the vanadium coordination also is almost square pyramidal. This correction was necessary to account for space charge effects. Hence the second peak was attributed to V^{IV} (516.2 eV). It is worth noting that the two peaks were refined with a same linewidth of 1.6 eV. Results of this deconvolution are shown in Figs. 6 and 7. Assuming an error margin of $\pm 3\%$ for the atomic percentages of the vanadium valences, average valence values of 4.47 ± 0.03 and 4.55 ± 0.03 were calculated respectively for octane- and hexanediamine templated vanadates. Although the XPS method more concerns surface analysis and can induce more uncertainty in chemical composition, the estimation obtained on the average valence state values seems to be in reasonable agreement with those calculated from the valence bond sums: 4.43 ± 0.02 and 4.60 ± 0.1. This latter value of 4.60 exhibits a higher uncertainty, most likely due to some degree of disorder in a large unit cell containing a high number of atoms.

An argument which strongly supports the ESCA analysis in two distributions, V^V and V^{IV}, in a cluster such as $[V_{15}O_{36}(Cl)]^{6-}$ templated by octanediamine arises from the determination of the electronic structure which is in progress (21). The eight electrons d^1 are distributed on very narrow levels built up from "t_{2g}" orbitals. For explaining the

TABLE 4
Sums of the Bond Valences for the V Atoms
$[NH_3(CH_2)_6NH_3]_{10}[V_{15}O_{37}(Cl)]_2[V_{15}O_{36}(Cl)](OH)_3(H_2O)_3$

Atom	Valence	Atom	Valence
	Cluster I: $[V_{15}O_{37}(Cl)]^{6-}$		
V(1)	4.59	V(9)	4.72
V(2)	4.83	V(10)	4.96
V(3)	4.87	V(11)	4.84
V(4)	4.94	V(12)	4.34
V(5)	4.57	V(13)	4.64
V(6)	4.21	V(14)	4.40
V(7)	4.68	V(15)	4.44
V(8)	4.26	Average Valence	4.62 ± 0.07
	Cluster II: $[V_{15}O_{36}(Cl)]^{5-}$		
V(16)	4.77	V(21)	4.24
V(17)	4.67	V(22)	4.52
V(18)	4.86	V(23)	4.46
V(19)	4.38	V(24)	3.74
V(20)	4.80	Average Valence	4.57 ± 0.10

Note. The results refer to the equation $\sum_i (d(V\text{–}O_i)/1{,}78)^{-5.15}$ (16).

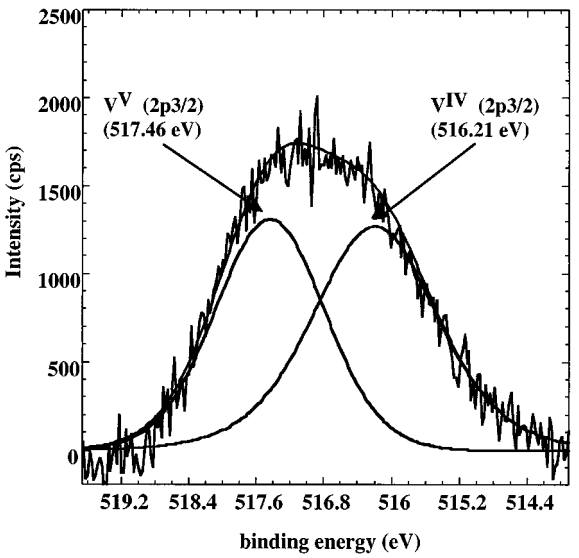

FIG. 6. XPS spectrum of V $2p_{3/2}$ and the result of deconvolution in two distributions: V^{V} and V^{IV} in $[NH_3(CH_2)_8NH_3]_3[V_{15}O_{36}(Cl)](NH_3)_6(H_2O)_3$.

evolution of the magnetic behavior depicted in Fig. 8, a model of magnetic insulator is proposed. It accounts for singly occupied levels with "spin up" and "spin down" states split by an exchange energy gap of about 0.2 eV. This model makes it possible to explain the magnetic moment value of 2.8 μ_B below 50 K, corresponding to two unpaired electrons, and accounts for the value of 4.9 μ_B at 300 K characteristic of four unpaired electrons. Naturally, when temperature is increased above 50 K, polaronic hopping between narrow levels increase more and more but filling of the different levels corresponds to half-filled or empty levels. So the redox V^{V}/V^{IV} is physically justified.

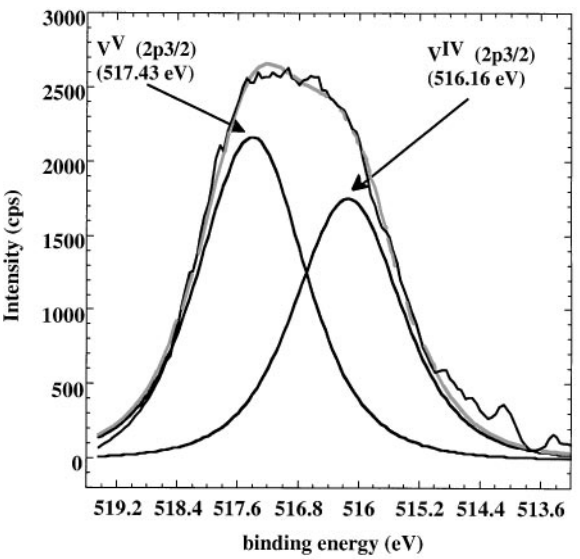

FIG. 7. XPS spectrum of V $2p_{3/2}$ and the result of deconvolution in two distributions: V^{V} and V^{IV} in $[NH_3(CH_2)_6NH_3]_{10}[V_{15}O_{37}(Cl)]_2[V_{15}O_{36}(Cl)](OH)_3(H_2O)_3$.

DISCUSSION

This study provides a novel example of organic–inorganic hybrid compound containing vanadium–oxygen clusters textured by alkyldiammonium cations. Diamines are considered as playing a double role: (a) reducing agent and (b) template. Although the mechanism of precipitation of clusters such as $[V_{15}O_{36}(Cl)]^{6-}$ or related is not known, it could be envisaged, in a first step, that at low pH values (~ 2.5), neutral monomeric vanadates species, reduced or not by diamines such as $[VO_2(OH)(H_2O)_3]$ or $[VO_2(OH)_2(H_2O)_2]$ (22), aggregate around Cl^- through dehydration and partial "oxolation" process to form oxohydroxylated clusters. In a second step, acid–base intercalation of diamines gives the mesostructured vanadate. Such an interpretation is possible since the clusters obtained by Shao *et al.* (17) with only ammonium and sodium cations exist without the templating effect.

Curiously, the diamine templates, as reducing species, lead, whatever the diamine, to mixed valence hybrids either with a particular value 4.5 found in layered vanadates (23–29) or with a value close to that value in hybrids with vanadium–oxygen clusters (octane- and hexanediamine). The mixed valence state in $(NH_4)_3Na_7[V_{15}O_{36}(Cl)]^{10-}$ $30H_2O$ (17) corresponds to 80% of V^{IV}. By considering different diamines, it appears that ethylendiamine is the most reducing one, as it reduces both V^{V} and Mo^{VI}, whose standard redox potentials are separated by 0.8 eV. That latter value was determined by estimation of the charge transfer gaps in UV–visible absorption spectra (≈ 2.20 eV for vanadium and 3.0 eV for molybdenum). The yield of the synthesis is about 85% for this diamine, whereas it is only 25% for dodecanediamine. Parallel to that tendency, the crystallinity decreases and single crystals are no longer formed. In order to have a best overview on the vanadate hybrids textured by diamines, we propose a phenomenological diagram with the standard redox potentials of Mo^{VI}/Mo^{V} and V^{V}/V^{IV} (symmetry C_{4v}) and a qualitative scale of "effective" redox potentials that have to account for all energies known or unknown in the different pathways that allow the synthesis of the hybrid (Fig. 9).

When reduction is thermodynamically allowed, kinetic effects can superpose even more when diamines are longer. Indeed viscosity plays an important role on intercalation in the second step proposed for the synthesis of these hybrids. So, small differences observed in the energy scale, could be dependent of kinetics of different decomposition pathways of diamines still unknown, according to the structural type.

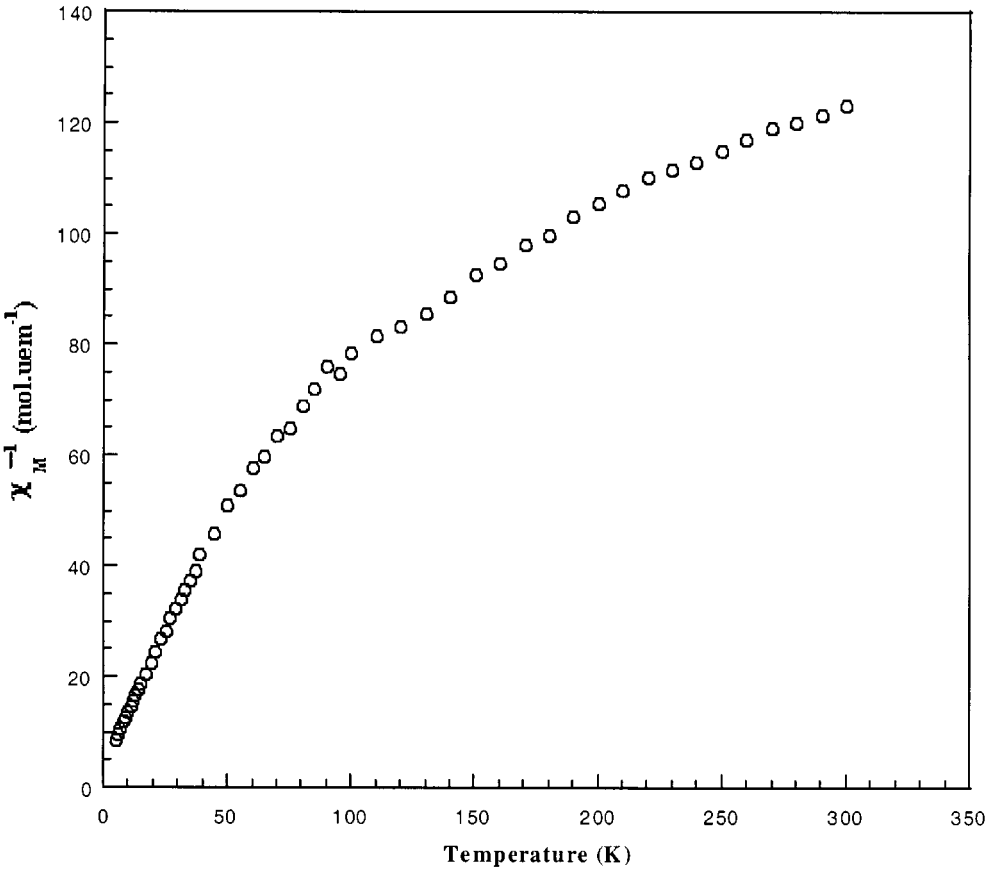

FIG. 8. Thermal evolution of the reciprocal molar susceptibility for $[NH_3(CH_2)_8NH_3]_3[V_{15}O_{36}(Cl)](NH_3)_6(H_2O)_3$.

The use of such a diagram was tested for diaminopropane on a mixture of MoO_3/V_2O_5, 1/1. Only a reduced vanadate hybrid was obtained.

Concerning the hexanediamine templated vanadate, no special attempt was made to change experimental conditions. On the contrary, they were chosen strictly similar to those selected for the synthesis of the octane compound, in order to make available comparisons. No ESR study has yet been done to test the behavior of the $[V_{15}O_{36}(Cl)]^{6-}$ cluster, but it is planned. A magnetic insulator behavior is also expected for the two clusters in the hexanediamine templated vanadate at low temperature, with a polaronic hopping at higher temperature.

CONCLUSION

The new mesostructured polyoxovanadate $[NH_3(CH_2)_6NH_3]_{10}[V_{15}O_{37}(Cl)]_2[V_{15}O_{36}(Cl)](OH)_3(H_2O)_3$ is another example of the templating effect of diamines. This organic–inorganic hybrid contains two types of clusters, $[V_{15}O_{36}(Cl)]^{5-}$ and $[V_{15}O_{37}(Cl)]^{6-}$, textured by organic dications, ensuring a cohesion with a different denseness. The less dense stacking inside the cell concerns the environment of $[V_{15}O_{36}(Cl)]^{5-}$ clusters between which channels with diameter size about 5.60 Å can adsorb free water molecules in addition to constituent water. The most compact part concerns the $[V_{15}O_{37}(Cl)]^{6-}$ clusters. So the structure has been described in terms of intergrowth of two sublattices with a two-dimensional character.

It is worth noting that the reducing power of diaminohexane seems to be slightly lower than that of diaminooctane according to the average valence state of vanadium, 4.60 ± 0.1 vs 4.43 ± 0.02, in reasonable agreement with those obtains by XPS experiments. These values, which depart slightly from the particular 4.5, result from an accomodation of mixed-valence state through occupation fluctuations of various narrow electronic levels inside the cluster. All the diamine templated vanadates exhibit magnetic properties which are those of magnetic insulators, at least at low temperature. They are either antiferromagnetic or magnetic insulators where "spin up" and "spin down" states are split by an exchange energy gap (0.2 eV in $[V_{15}O_6(Cl)]^{6-}$). After analysis of different results found in the literature, the shorter diamines rather induce layered structures, whereas the longer favor clustering of the vanadate framework.

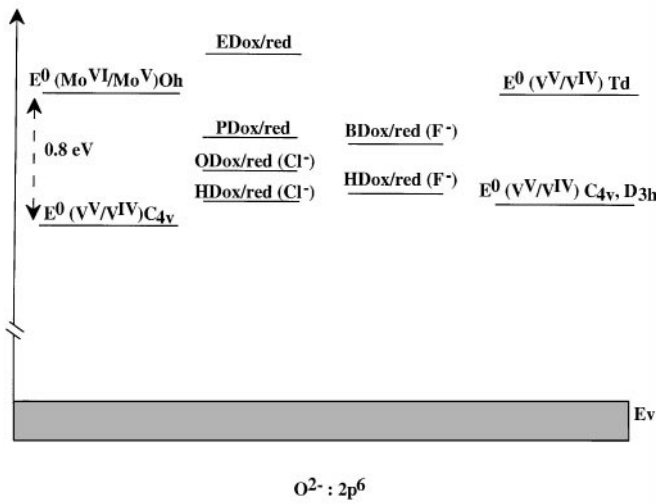

FIG. 9. Phenomenological diagram implying "effective" redox potential of diamines (ED, ethylenediamine; PD, propanediamine; BD, butanediamine; HD, hexanediamine; OD, octanediamine) placed with regard to the standard redox couples V^V/V^{IV} in different site symmetries and Mo^{VI}/Mo^V in Oh symmetry.

From all these results, we have proposed the concept of "effective" redox potential of diamines to account for all energies, known or unknown, contributing to their apparent reducing power. The thermodynamic component is always present but can be superposed to kinetic contributions of different pathways affecting especially the longer diamines. The "effective" redox potentials have been placed on a scale which is compared to the standard redox potentials Mo^{VI}/Mo^V and V^V/V^{IV}. Because the mean valence state of vanadium is always close to 4.5, it is expected that the position of the longer diamines in the scale rather reflects kinetic contributions. Other experiments are in progress to improve our knowledge on the thermodynamics of those complex systems.

REFERENCES

1. R. M. Barrer, "Hydrothermal Chemistry of Zeolites." Academic Press, London, 1982.
2. R. Szostak, "Moleculmar Sieves—Principles of Synthesis and Identification." Van Nostrand–Reinhold, New York, 1989.
3. J. S. Beck, J. C. Vartuli, W. J. Roth, M. E. Leonowicz, C. T. Kresge, K. D. Schmitt, C. T-W Chu, D. H. Olson, E. W. Sheppard, S. B. McCullen, J. B. Higgins, and J. L. Schlenker, *J. Am. Chem Soc.* **114,** 10,834 (1992).
4. C. T. Kresge, M. E. Leonowicz, J. C. Vartuli, and J. S. Beck, *Nature* **359,** 710 (1992).
5. R. C. Haushalter and L. A. Mundi, *Chem. Mater.* **4,** 31 (1992).
6. V. Soghomonian, R. C. Haushalter, Q. Chen, and J. Zubieta, *Inorg. Chem.* **33,** 1700 (1994).
7. V. Soghomonian, Q. Chen, R. C. Haushalter, J. Zubieta, C. J. O'Connor, and Y. S. Lee, *Chem. Mater.* **5,** 1690 (1993).
8. M. I. Khan, Y. S. Lee, C. J. O'Connor, R. C. Haushalter, and J. Zubieta, *Inorg. Chem.* **33,** 3855 (1994).
9. V. Soghomonian, Q. Chen, R. C. Haushalter, J. Zubieta, and C. J. O'Connor, *J. Sci.* **259,** 1596 (1993).
10. V. Soghomonian, Q. Chen, R. C. Haushalter, and J. Zubieta, *Angew. Chem. Int. Ed. Engl.* **32,** 610 (1993).
11. Y. Zhang, A. Clearfield, and R. C. Haushalter, *Chem. Mater.* **7,** 1221 (1995); *J. Solid State Chem.* **117,** 157 (1995).
12. N. Guillou, G. Férey, and M. S. Whittingham, *J. Mater. Chem.* **8**(10), 2277 (1998).
13. T. Drezen, O. Joubert, M. Ganne, and L. Brohan., *J. Solid State Chem.* **136,** 298 (1998).
14. T. Drezen, Thesis, Nantes, France, 1998.
15. A. Müller, E. Krickemeyer, M. Penk, R. Rohlfing, A. Armatage, and H. Bögge, *Angew. Chem. Int. Ed. Engl.* **8,** 926 (1990).
16. A. Müller, M. Penk, R. Rohlfing, E. Krickemeyer, and J. Döring, *Angew. Chem. Int. Ed. Engl.* **42,** 1674 (1991).
17. M. Shao, J. Leng, Z. Pan, H. Zeng, and Y. Tang, *Gaogeng Xuexiao Huaxue Xuebao KTHPD* **11,** 280 (1990)
18. G. M. Sheldrick, SHELXTL version 5, Siemens Analytical X-Ray Instruments, Inc., Madison, WI, 1995.
19. I. D. Brown and D. Altermatt, *Acta Crystallogr. Sect. B* **41,** 244 (1985).
20. C. D. Wagner, W. M. Riggs, L. E. Davis, J. F. Moulder, and G. E. Muilenberg (Eds.), "Handbook of X-Ray Photoelectron Spectroscopy." Perkin–Elmer Corp., MI, 1978.
21. H. J. Koo, M. H. Whangbo, T. Drezen, and M. Ganne, in preparation.
22. J. P. Jolivet, "De la Solution à L'Oxyde. InterEdition/CNRS Editions, Paris, 1994.
23. D. Riou and G. Férey, *Inorg. Chem.* **34,** 6520 (1995).
24. D. Riou and G. Férey, *J. Solid State Chem.* **120,** 137 (1995).
25. L. F. Nazar, B. E. Koene, and J. F. Britten, *Chem. Mater.* **8,** 327 (1996)
26. C. Ninclaus, D. Riou, and G. Férey, *Acta Crystallogr. Sect. C* **52,** 512 (1996).
27. D. Riou and G. Férey, *J. Solid State Chem.* **124,** 151 (1996).
28. Y. Zhang, R. C. Haushalter, and A. Clearfield, *Inorg. Chem.* **35,** 4950 (1996).
29. Y. Zhang, C. J. O'Connor, A. Clearfield, and R. C. Haushalter, *Chem. Mater.* **8,** 595 (1996).